Article

Not peer-reviewed version

Goat Whey Protein Hydrolysate Mitigates High-Fructose Corn Syrup-Induced Hepatic Steatosis in a Murine Model

Chun-Hui Shao , Vipul Wayal * , Chang-Chi Hsieh *

Posted Date: 9 April 2025

doi: 10.20944/preprints202504.0794.v1

Keywords: Goat whey protein hydrolysate; Hepatic steatosis; High-fructose corn syrup; Bioactive peptides; Ketohexokinase; Glucose homeostasis

 doi:10.20944/preprints202504.0794.v1

Article

Goat Whey Protein Hydrolysate Mitigates High-Fructose Corn Syrup-Induced Hepatic Steatosis in a Murine Model

Chun-Hui Shao [1,2], Vipul Wayal [1,*] and Chang-Chi Hsieh [1,*]

[1] Department of Animal Science and Biotechnology, Tunghai University, Taichung 407224, Taiwan

[2] Department of Pharmacy, Central Clinic & Hospital, Taipei 106441, Taiwan

* Correspondence: wayalvipul9704@gmail.com (V.W.); cchsieh@thu.edu.tw (C.-C.H.)

Abstract: Hepatic steatosis, characterized by abnormal fat accumulation in the liver, is a major health concern with limited effective treatments. Goat milk whey proteins have demonstrated various therapeutic benefits. This study aimed to evaluate the hepatoprotective effects of goat whey protein hydrolysate (GWPH) on high-fructose corn syrup (HFCS)-induced hepatic steatosis in a murine model. GWPH was prepared through enzymatic hydrolysis using Alcalase® and divided into fractions: GWPH03 (<3 kDa), GWPH0310 (3–10 kDa), GWPH1030 (10–30 kDa), and GWPH30 (>30 kDa). These fractions were administered to respective GWPH treatment groups at 200 mg/kg b.w/day via intragastric gavage for 8 weeks, with HFCS provided to all groups except the Naïve group. After dietary intervention, an oral glucose tolerance test (OGTT) was performed, and mice were sacrificed for further analysis. Our results demonstrate that GWPH mitigates HFCS-induced hepatic steatosis, reduces body weight gain, improves glucose homeostasis, alleviates liver injury, and regulates hepatic lipid metabolism. Molecular docking of identified peptides from GWPH, particularly PFNVYNVV, which showed strong binding affinity for KHK, suggesting its potential as a competitive inhibitor of fructose metabolism. Collectively, these findings suggest that GWPH and its derived peptides could be promising candidates for managing hepatic steatosis and related metabolic abnormalities.

Keywords: goat whey protein hydrolysate; hepatic steatosis; high-fructose corn syrup; bioactive peptides; Ketohexokinase; glucose homeostasis

1. Introduction

Liver is a vital metabolic organ involved in protein, fat, and carbohydrate metabolism. Impaired liver function can lead to chronic liver diseases, cirrhosis, liver cancer, and metabolic disorders. Among these, hepatic steatosis or excessive fat accumulation in the liver, is a major health concern [1,2]. When liver fat accumulates and increases total liver weight by 5%, it is called hepatic steatosis or fatty liver, and most fatty livers are associated with metabolic syndrome, including obesity, diabetes, hyperlipidemia, and various cardiovascular abnormalities [3]. Hepatic steatosis affects approximately 25% of the global population, with prevalence rising due to increasing obesity and metabolic syndrome. It is particularly common in developed countries, where sedentary lifestyles and high-caloric diets contribute to their growing burden [4]. Fatty liver, previously known as non-alcoholic fatty liver disease (NAFLD), has been reclassified in 2023 as metabolic dysfunction-associated steatotic liver disease (MASLD) to emphasize its strong association with metabolic dysfunction [5]. Hepatic steatosis is graded by fat accumulation in hepatocytes: Grade 0 (<5%, normal), Grade 1 (5%–33%, mild), Grade 2 (34%–66%, moderate), and Grade 3 (>66%, severe) [4].

High fructose intake is strongly linked to hepatic steatosis due to its distinct hepatic metabolism. Unlike glucose, fructose bypasses key regulatory steps and is rapidly phosphorylated by ketohexokinase (KHK) to fructose-1-phosphate, leading to ATP depletion and unregulated entry into

 doi:10.20944/preprints202504.0794.v1

lipid synthesis pathways [6]. This accelerates hepatic lipogenesis, promoting excessive triglyceride (TG) accumulation and fat deposition in the liver. Excessive fructose consumption contributes to insulin resistance, oxidative stress, and inflammation, exacerbating hepatic lipid accumulation and increasing the risk of steatohepatitis and MASLD [7,8]. Given the central role of KHK in fructose metabolism, modulating its activity may provide a potential strategy for alleviating HFCS-induced hepatic steatosis and its associated metabolic complications [9]. Previous studies indicate that high-fructose corn syrup (HFCS) consumption further accelerates hepatic steatosis progression by promoting lipogenesis and impairing metabolic homeostasis. Widely used in processed foods, soft drinks, and beverages, HFCS contains high levels of fructose and has been strongly associated with obesity and metabolic disorders. Notably, HFCS can induce metabolic syndrome-related alterations independent of weight gain, underscoring its role in the global rise of obesity, insulin resistance, and cardiovascular diseases [10–12].

Despite advancements in metabolic disease management, there are currently no FDA-approved pharmacological treatments specifically for hepatic steatosis. Existing therapeutic approaches primarily focus on lifestyle modifications, while available pharmacologic options, such as insulin sensitizers and lipid-lowering agents, often have limited efficacy and potential adverse effects [13]. Given these challenges, there is a growing interest in functional food ingredients, including bioactive proteins, protein hydrolysates and bioactive peptides and natural bioactive compounds with hepatoprotective properties [14–17].

Goat milk, often considered a superior alternative to cow milk, has gained attention for its potential health benefits. Specifically, whey proteins from goat milk have been found to offer numerous therapeutic advantages and health-promoting effects, including their immunomodulatory effects, potential for allergy management, anti-inflammatory and antioxidant activities, as well as their antimicrobial and anticancer properties [18]. In prior study suggested that the enzymatic hydrolysis of whey proteins using proteases generates low-molecular-weight bioactive fractions, which may serve as potential candidates for mitigating conditions such as atherosclerosis and hepatic steatosis. Additionally, these whey protein hydrolysate fractions exhibit promising cardioprotective properties, highlighting their potential as novel functional ingredients for the management of cardiovascular diseases (CVD) [19]. Furthermore, a recent study evaluated the *in vitro* biosafety and bioactivity of goat milk protein-derived hydrolysates, demonstrating their potential as functional ingredients. Casein and whey proteins were enzymatically hydrolyzed to generate gastrointestinal-stable peptides, which exhibited significant inhibitory activity against α-amylase, pancreatic lipase, and angiotensin-converting enzyme, along with antibacterial and immunomodulatory properties. Cytotoxicity analysis confirmed their safety, highlighting goat milk protein hydrolysates as promising candidates for nutraceutical and functional food applications [20].

However, a comprehensive evaluation of the impact of goat whey protein hydrolysate (GWPH) on hepatic steatosis remains lacking. Additionally, no studies have yet established a direct link between GWPH and hepatic steatosis. Therefore, this study aims to investigate the hepatoprotective effects of GWPH in a murine model of HFCS-induced hepatic steatosis and elucidate its underlying mechanisms.

2. Materials and Methods

2.1. Chemicals and Reagents

Alcalase® protease enzyme (≥ 2.4 U/g specific activity) and Rennet (≥4% protein) was purchased from Sigma-Aldrich Co. LLC. (St. Louis, MO, USA). Pierce® BCA Protein Assay kit was purchased from Thermo Fisher Scientific (Waltham, MA, USA). HFCS was purchased from Fonen and Fonher Enterprise Co., Ltd. (Tainan City, Taiwan). CareSens™ II Blood Glucose Monitoring System purchased from i-SENS Inc. (Seoul, Korea). D-glucose was from Sigma-Aldrich Co. LLC. (St. Louis, MO, USA). Alanine aminotransferase (ALT), aspartate aminotransferase (AST), triglycerides (TG),

 doi:10.20944/preprints202504.0794.v1

and total cholesterol (TC) Cobas assay kits were purchased from Roche Diagnostics Ltd. (Taipei, Taiwan).

2.2. Collection of Goat Milk Sample

Goat milk samples were obtained from Yi Jian Dairy Sheep Farm (Taichung City, Taiwan). Freshly collected milk was immediately chilled to 4 °C to prevent microbial growth and transported to laboratory under cold conditions.

2.3. Preparation of Goat Whey Protein (GWP)

Raw goat milk was pasteurized by indirect heating in a water bath at 62–65 °C with continuous stirring for 20 minutes. After pasteurization, the milk was cooled to 35 °C, and citric acid (3 g/L) was added to adjust the pH to approximately 4.0–5.0. The mixture was allowed to stand for 20 minutes and then rennet (0.4 g per 5 L of milk) was added dropwise to further facilitate coagulation, and mixture was left undisturbed for 30 minutes at room temperature. After a 30-minute incubation period, the coagulated curd was separated from the whey by filtration through muslin cloth. The resulting whey was collected and referred to as GWP. Protein concentration in GWP was determined using BCA protein assay, following the manufacturer's instructions.

2.4. Preparation of Goat Whey Protein Hydrolysate (GWPH)

Enzymatic hydrolysis of GWP was performed using 1% Alcalase® protease enzyme at 55 °C for 6 hours to obtain GWPH. After hydrolysis, the reaction mixtures were filtered through glass wool to remove particulates and centrifuged at 10,000 × *g* for 30 minutes at 4 °C. The supernatants were collected and filtered sequentially through 0.45 µm and 0.22 µm membrane filters. Size-based fractionation was performed using centrifugal ultrafiltration tubes with molecular weight cut-offs of 30 kDa, 10 kDa, and 3 kDa, yielding the following hydrolysate fractions: GWPH03 (<3 kDa), GWPH0310 (3–10 kDa), GWPH1030 (10–30 kDa), and GWPH30 (>30 kDa). Each fraction was collected and stored at –20 °C until further analysis.

2.5. Identification of Bioactive Peptides from GWPH Using LC-MS/MS De Novo Sequencing

The peptide profiles of GWPH fractions (<3 kDa, 3–10 kDa, and 10–30 kDa) were analyzed using liquid chromatography–tandem mass spectrometry (LC-MS/MS). GWPH samples were desalted on a Zorbax 300SB C18 column (Agilent Technologies, CA, USA) and separated on a Waters BEH C18 column (1.7 µm, 100 µm × 10 cm). with a 70 min gradient of acetonitrile (0.1% formic acid) at 0.3 µL/min. MS analysis was conducted using an Orbitrap Elite ETD mass spectrometer (Thermo Fisher Scientific, MA, USA). Peptide identification was performed using Proteome Discoverer (Mascot, UniProt) and *de novo* sequencing with PEAKS Studio v10.5 (Bioinformatics Solutions Inc., ON, Canada), with a 10 ppm precursor and 0.1 Da fragment ion tolerance. Peptides were filtered to FDR < 1% and ALC ≥ 50%. Fractions <30 kDa were prioritized due to their higher abundance and bioactivity potential.

2.6. Animals and Experimental Design

A total of 60 six-week-old male C57BL/6JNarl mice were procured from National Laboratory Animal Center (NAR labs; Taipei, Taiwan). The mice were maintained on a 12-hour light/dark cycle at a temperature of 22–25°C and humidity of 45–60% during a one-week acclimatization period. They were provided with a standard chow diet purchased from Altromin Spezialfutter GmbH & Co. KG (Lage, Germany) and distilled water ad libitum. After one week of acclimatization, mice were weighed to record for initial body weight and randomly assigned into six groups (n=10 per group). Naïve group fed with normal chow diet without any treatment and provided with distilled water. Control group received a standard chow diet supplemented with HFCS (30% v/v) in drinking water bottles, along with sterile distilled water (10 mL/kg.bw/day) administered via intragastric gavage.

 doi:10.20944/preprints202504.0794.v1

The remaining four groups also received HFCS (30% v/v) in their drinking water bottles and were treated with different molecular weight fractions of GWPH at a dose of 200 mg/kg.bw/day. These groups included GWPH03 (GWPH fraction <3 kDa), GWPH0310 (GWPH fraction 3–10 kDa), GWPH1030 (GWPH fraction 10–30 kDa), and GWPH30 (GWPH fraction >30 kDa). The body weight of mice was recorded weekly.

At the end of 8 weeks, mice were kept for overnight fasting and the final body weight was recorded. Percentage body weight gain = final bw (g) – initial bw (g) / initial bw (g) × 100 %. Then, fasting blood glucose (FBG) and oral glucose tolerance test (OGTT) were performed. Blood samples were collected, and mice were euthanized by isoflurane inhalation. The livers and visceral white adipose tissues, including epididymal and perirenal white adipose tissues, were carefully dissected and weighed. Liver index was calculated as liver weight (g) / final bw (g) × 100 %. Animal experimental procedures were approved by the Institutional Animal Care and Use Committee (IACUC) of Tunghai University, Taiwan (Ethical approval number: 102-020, 104-020).

2.7. FBG and OGTT

At the end of the 8th week of dietary intervention, mice were fasted overnight. Blood was obtained from caudal tail vein and FBG levels were measured using CareSens™ II Blood Glucose Monitoring System. FBG reading was considered as the '0-minute' blood glucose level for the OGTT. After FBG measurement, mice were administered D-glucose (2 g/kg. bw) via intragastric gavage, and blood glucose levels were subsequently recorded at 30, 60, 90, 120, and 150 minutes. The area under the blood glucose curve (AUC) was then calculated to assess glucose tolerance.

2.8. Determination of Serum and Liver Biochemical Parameters

Serum levels of ALT and AST were measured using UV spectrophotometric method with Cobas ALT and AST assay kits. Serum TG, and TC contents were determined using enzymatic colorimetric method with Cobas TG and TC kits. All assays were performed according to the manufacturer's instructions. Similarly, hepatic TG levels were measured in liver homogenates. Very low-density lipoprotein (VLDL) levels in both serum and liver were calculated using Friedewald formula, defined as 1/5th of TG level [21,22].

2.9. Histopathological Examination

Fresh liver tissue specimens were fixed in a 10% neutral buffered formalin solution. The fixed tissues were then embedded in paraffin wax, sectioned into 5-µm slices, and stained with hematoxylin and eosin (H&E). The stained sections were examined under a Nikon ECLIPSE E200 microscope (Nikon Corporation, Tokyo, Japan), and photomicrographs were captured. The obtained photomicrographs were subsequently analyzed and compared to assess hepatic steatosis.

2.10. Molecular Docking Analysis of Bioactive Peptides from GWPH for KHK Inhibition

Molecular docking was performed according to a previous study by Wayal et al., (2025), to evaluate the binding affinity of selected GWPH-derived peptides against KHK, a key enzyme involved in fructose metabolism [23]. The crystal structure of human KHK (PDB ID: 2HLZ) was obtained from the RCSB Protein Data Bank, with structural details shown in Figure S6. Docking was performed using AutoDock 4.2 software [24], and binding interactions were visualized using BIOVIA Discovery Studio visualizer [25].

2.11. Statistical Analysis

Data are presented as means ± SD. Multiple group comparisons were performed using one-way ANOVA, followed by Duncan's post-hoc test. p-value < 0.05 was considered statistically significant. All statistical analyses were conducted using SPSS 26.0 software (IBM, Chicago, IL, USA)

 doi:10.20944/preprints202504.0794.v1

3. Results

3.1. Identification of Selected Bioactive Peptides from GWPH

Several bioactive peptides were identified from different molecular weight fractions (<3 kDa, 3–10 kDa, and 10–30 kDa) of GWPH using LC-MS/MS analysis. Peptides from <3 kDa fraction demonstrated the highest relative abundance, with Lys-Tyr-Asp-Ser-Val-Leu-Ala-Val (KYDSVLAV) and Glu-Pro-Gln-Leu-His-Pro-Phe (EPQLHPF) representing 4.01% and 3.31%, respectively. In 3–10 kDa fraction, Ala-Ser-His-Pro-Asp-Leu-Asn-Val-Val (ASHPDLNVV) and Thr-Pro-Val-Val-Val-Pro-Pro-Phe (TPVVVPPF) were identified with relative abundances of 3.03% and 2.84%, respectively. Peptides from the 10–30 kDa fraction, Pro-Phe-Asn-Val-Tyr-Asn-Val-Val (PFNVYNVV), exhibited a relative abundance of 2.52%. These peptides were selected for further investigation based on their prevalence, structural properties, and potential for bioactivity.

3.2. Effect of GWPH on Physiological Indicators in HFCS-Fed C57BL/6J Mice

After 8 weeks of HFCS feeding, Control group exhibited significantly higher body weight, liver weight, and increased visceral adiposity in eWAT and prWAT compared to Naïve group ($p < 0.05$, Table 1). Among the GWPH-treated groups for 8 weeks, GWPH1030 and GWPH30 significantly reduced body weight compared to Control group ($p < 0.05$), while no significant changes were observed in GWPH03 and GWPH0310 groups. Liver weights were significantly lower in all GWPH-treated groups compared to the Control group ($p < 0.05$). Visceral adiposity in eWAT and prWAT was significantly reduced in all GWPH treatment groups except GWPH03 ($p < 0.05$).

As illustrated in Figure 1A, the Control group exhibited significantly higher body weight gain compared to the Naïve group ($p < 0.05$), whereas all GWPH-treated groups demonstrated a significant reduction in body weight gain compared to Control group ($p < 0.05$). The liver index (wet liver weight-to-final body weight ratio) was elevated in the Control group, with no significant difference from the Naïve group. However, GWPH03, GWPH0310, and GWPH1030 treatments significantly lowered the liver index compared to the Control group, while GWPH30 did not show a significant difference ($p < 0.05$, Figure 1B).

Table 1. Effect of GWPH on physiological indicators in HFCS-fed C57BL/6J mice.

Physiological Indicators	Naïve (Untreated)	HFCS-Induced Hepatic Steatosis				
		Control	GWPH03	GWPH0310	GWPH1030	GWPH30
Initial BW (g)	22.29 ± 1.25	22.48 ± 1.01	22.19 ± 1.56	22.30 ± 1.30	21.86 ± 0.94	22.18 ± 1.12
Final BW (g)	26.29 ± 1.46 ^{a}	30.91 ± 1.90 ^{c}	29.57 ± 2.05 ^{bc}	29.56 ± 1.62 ^{bc}	28.49 ± 1.42 ^{b}	28.78 ± 3.25 ^{b}
Liver wt. (g)	1.074 ± 0.091 ^{a}	1.223 ± 0.076 ^{b}	1.087 ± 0.091 ^{a}	1.124 ± 0.047 ^{a}	1.075 ± 0.060 ^{a}	1.121 ± 0.142 ^{a}
eWAT wt. (g)	0.366 ± 0.076 ^{a}	1.004 ± 0.362 ^{c}	0.801 ± 0.256 ^{b}	0.736 ± 0.101 ^{b}	0.724 ± 0.170 ^{b}	0.729 ± 0.237 ^{b}
prWAT wt. (g)	0.118 ± 0.072 ^{a}	0.320 ± 0.085 ^{c}	0.252 ± 0.103 ^{bc}	0.233 ± 0.050 ^{b}	0.185 ±0.049 ^{ab}	0.231 ± 0.129 ^{b}

* Data are expressed as mean ± SD (n = 10). Different superscript letters (a, b, c) within the same row indicate significant differences between groups ($p < 0.05$).

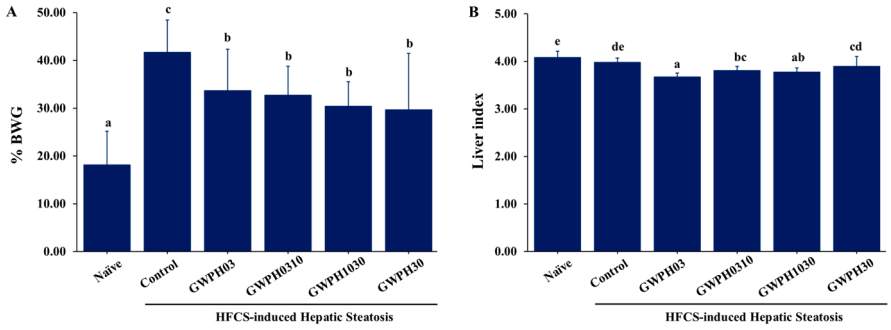

Figure 1. GWPH reduced body weight gain and liver index in HFCS-fed C57BL/6J mice: **(A)** Percentage body weight gain; **(B)** liver index. Data are expressed as mean ± SD (n = 10). Different superscript letters (a, b, c, d, e) indicate significant differences between groups ($p < 0.05$).

 doi:10.20944/preprints202504.0794.v1

3.3. Effect of GWPH on Serum Biochemical Parameters in HFCS-Fed C57BL/6J Mice

Liver injury in HFCS-fed C57BL/6J mice were assessed by measuring serum levels of liver injury markers including ALT and AST. In comparison to the Naïve group, ALT and AST levels was significantly elevated in the Control group ($p < 0.05$). Notably, GWPH treatment significantly reduced these levels, showing a marked improvement in liver injury. ALT and AST levels in GWPH-treated groups were significantly lower than in the Control group and showed no significant difference from the Naïve group ($p < 0.05$, Figure 2A), except for AST levels in the GWPH30 group, which remained comparable to the Control group.

In the serum lipid profile, as shown in Figure 2B, serum levels of TG, TC, and VLDL were significantly higher in the Control group compared to the Naïve group ($p < 0.05$). However, GWPH treatment did not significantly affect serum TG, TC, or VLDL levels compared to the Control group, except for the GWPH30 group, which showed a significant reduction in TC levels ($p < 0.05$).

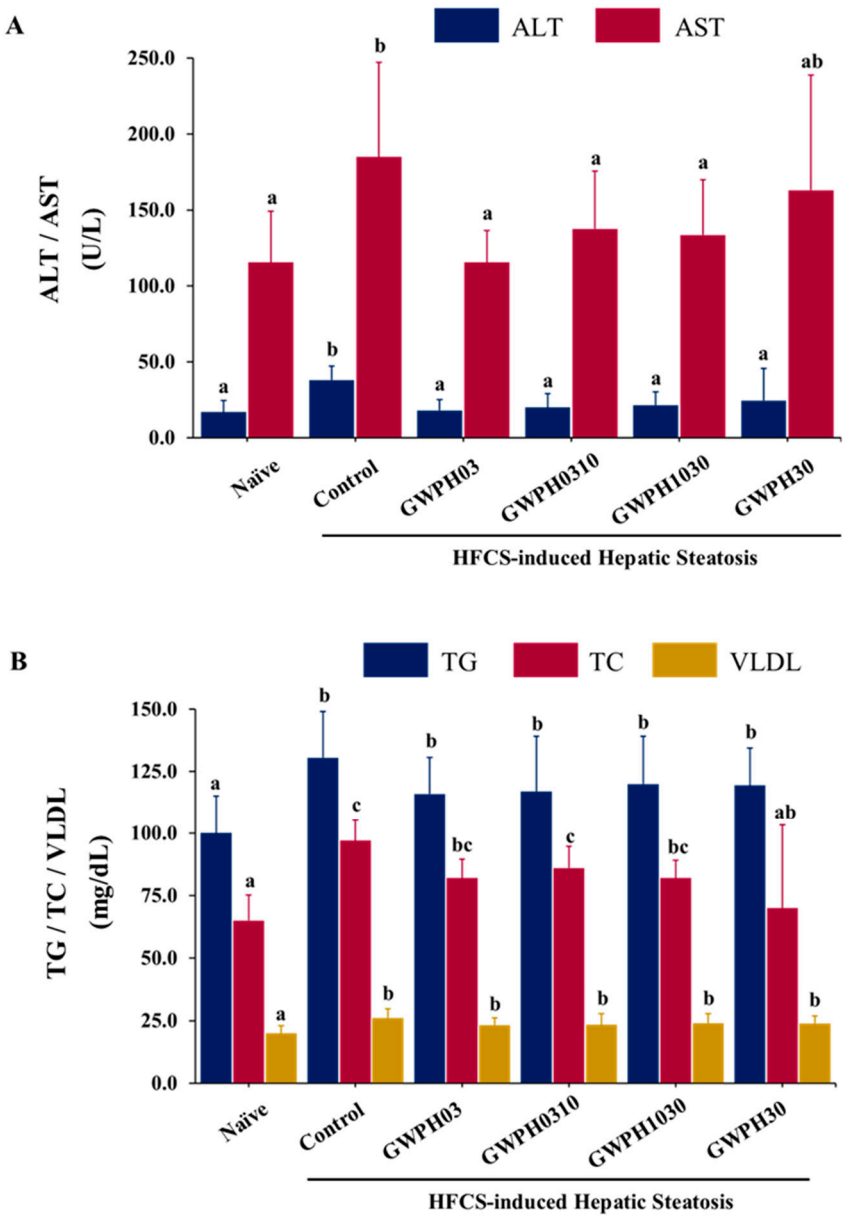

Figure 2. Effect of GWPH on serum biochemical parameters in HFCS-fed C57BL/6J mice: **(A)** Serum levels of liver injury markers: ALT and AST; **(B)** serum lipid profile: TG, TC and VLDL levels. Data are expressed as mean ± SD (n = 10). Different superscript letters (a, b, c) indicate significant differences between groups ($p < 0.05$).

 doi:10.20944/preprints202504.0794.v1

3.4. Effect of GWPH on Glucose homeostasis in HFCS-Fed C57BL/6J Mice

Long-term HFCS consumption resulted in a significant elevation of FBG levels, impaired glucose tolerance and an increased AUC for OGTT in the Control group mice compared to mice without HFCS feeding in Naïve group ($p < 0.05$, Figure 3A-C). In contrast, GWPH dietary intervention for 8 weeks alongside HFCS intake significantly reduced FBG levels in all treated groups, except for the GWPH0310 group, compared to Control group ($p < 0.05$, Figure 3A). Additionally, all GWPH-treated groups showed improved glucose tolerance in the OGTT, as reflected by lower glucose levels compared to Control group ($p < 0.05$, Figure 3B). Moreover, GWPH treatment significantly decreased AUC of the OGTT compared to Control group, indicating a significant improvement in glucose homeostasis ($p < 0.05$, Figure 3C).

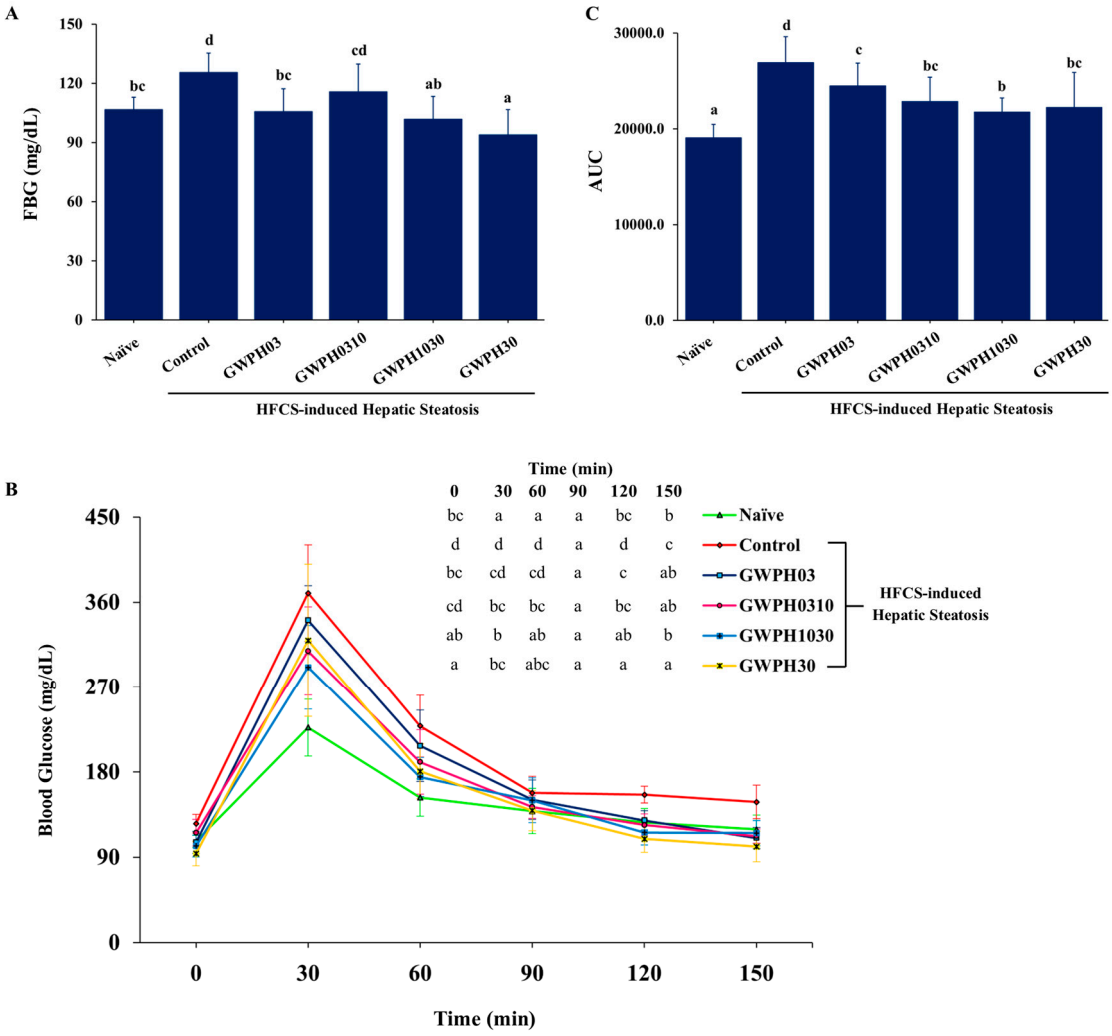

Figure 3. Effect of GWPH on glucose homeostasis in HFCS-fed C57BL/6J mice: **(A)** FBG levels; **(B)** OGTT; **(C)** AUC of OGTT. Data are expressed as mean ± SD (n = 10). Different superscript letters (a, b, c, d) indicate significant differences between groups ($p < 0.05$). In the OGTT graph **(B)**, superscript letters within the same column at each time point (0, 30, 60, 90, 120, and 150 minutes) indicate significant differences between groups ($p < 0.05$).

3.5. Effect of GWPH on Liver Lipid Levels and Hepatic Steatosis in HFCS-Fed C57BL/6J Mice

Chronic intake of HFCS resulted high fat accumulation and severe hepatic steatosis, as evidenced by significant changes in liver gross morphology and histopathology in Control group compared to Naïve group (Figure 4A-C). However, GWPH treatment groups including GWPH03 and GWPH1030 significantly alleviated hepatic steatosis and reversed the morphological alterations

 doi:10.20944/preprints202504.0794.v1

observed in the liver compared to Control group (Figure 4A, B). As shown in Figure 4C, Control group exhibited, higher levels of hepatic TG and VLDL compared to Naïve group ($p < 0.05$). In contrast, GWPH-treated groups, particularly GWPH1030, demonstrated a significant reduction in hepatic TG and VLDL levels compared to Control group ($p < 0.05$).

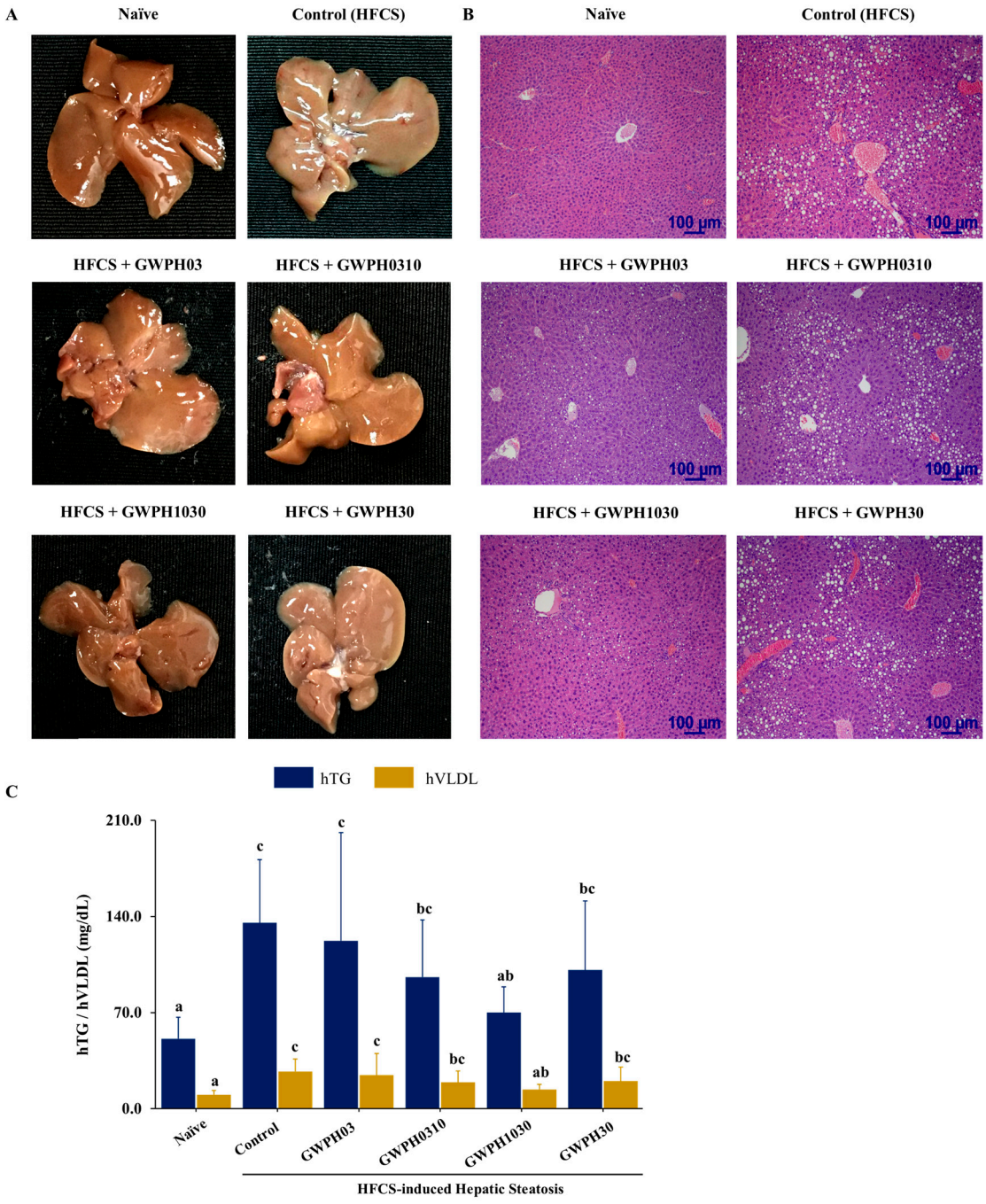

Figure 4. Effect of GWPH on hepatic lipid levels and hepatic steatosis in HFCS-fed C57BL/6J mice: **(A)** Liver gross morphology; **(B)** histopathological analysis of liver tissue using H&E staining (magnification: 100×, scale bar: 100 μm); **(C)** hepatic lipid profile: hTG and hVLDL levels. Data are expressed as mean ± SD (n = 10). Different superscript letters (a, b, c) indicate significant differences between groups ($p < 0.05$).

 doi:10.20944/preprints202504.0794.v1

3.6. Molecular Docking of Selected GWPH Peptides for KHK Inhibition

Five peptides (KYDSVLAV, EPQLHPF, ASHPDLNVV, TPVVVPPF and PFNVYNVV) selected from different molecular weight fractions of GWPH, were evaluated for their inhibitory potential against KHK using molecular docking. The 3D structures of these peptides (Figure S1–S5) were prepared as ligands, while the crystal structure of KHK (PDB ID: 2HLZ) was used as target protein, both prepared in docking PDB format using BIOVIA Discovery Studio. The results were compared with those reported by Zhu et al. (2023), wherein Compound 14 (KHK-IN-4) was identified as a potent KHK inhibitor [26]. The docking of Compound 14 with KHK served as a reference docking in present study.

All five peptides exhibited distinct binding energies, docking poses and key interactions with active site residues toward KHK (Table 2, Figures 5–7). In principle, lower the binding energies suggest stronger binding affinity. Notably, PFNVYNVV demonstrated the strongest binding affinity, with a binding energy of –9.6 kcal/mol, surpassing that of Compound 14, suggesting a potentially more robust interaction. Moreover, PFNVYNVV displayed a docking pose and interaction profile that closely resembled that of Compound 14 (Table 2 and Figure 7), further underscoring its potential as a competitive KHK inhibitor.

Table 2. Binding energies and docking interaction profile of GWPH-derived peptides and Compound 14 with KHK.

Compound 14	**KYDSVLAV**	**EPQLHPF**	**ASHPDLNVV**	**TPVVVPPF**	**PFNVYNVV**
ΔG = -9.5 kcal/mol	-8.0 kcal/mol	-9.7 kcal/mol	-9.6 kcal/mol	-9.4 kcal/mol	-9.6 kcal/mol
ASN42	ASN42	ASN42	ASN42	ASN42	ASN42
ARG108	ARG108	ARG108	ARG108	ARG108	ARG108
GLU173	GLU173	GLU173	GLU173	GLU173	GLU173
SER192	SER192	SER192	SER192	SER192	SER192
LYS193	LYS193	LYS193	LYS193	LYS193	LYS193
ASP194	ASP194	ASP194	ASP194	-	ASP194
ALA224	ALA224	ALA224	ALA224	ALA224	ALA224
ALA226	ALA226	ALA226	ALA226	ALA226	ALA226
ALA230	-	-	-	-	ALA230
PHE245	PHE245	PHE245	PHE245	-	PHE245
PRO247	-	-	PRO247	PRO247	PRO247
VAL250	-	-	-	VAL250	VAL250
THR253	THR253	THR253	THR253	THR253	THR253
GLY255	GLY255	GLY255	GLY255	GLY255	GLY255
ALA256	ALA256	ALA256	ALA256	ALA256	ALA256
GLY257	GLY257	GLY257	GLY257	GLY257	GLY257
ASP258	ASP258	ASP258	ASP258	ASP258	ASP258
PHE260	PHE260	PHE260	PHE260	PHE260	PHE260
CYS282	CYS282	CYS282	CYS282	-	CYS282
ALA285	ALA285	ALA285	ALA285	ALA285	ALA285

* ΔG, binding energy. Lower binding energies (or more negative values) indicate stronger binding affinity.

 doi:10.20944/preprints202504.0794.v1

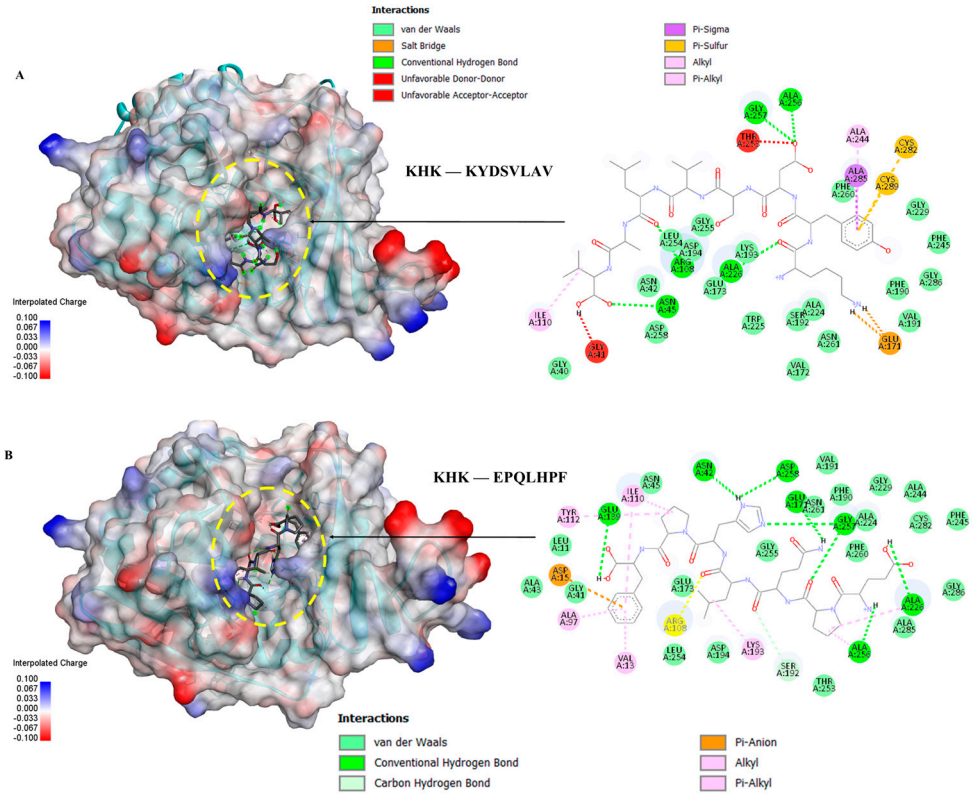

Figure 5. Molecular docking of peptides KYDSVLAV and EPQLHPF with KHK: **(A)** Binding pose and docking interactions of KYDSVLAV with KHK; **(B)** binding pose and docking interactions of EPQLHPF with KHK.

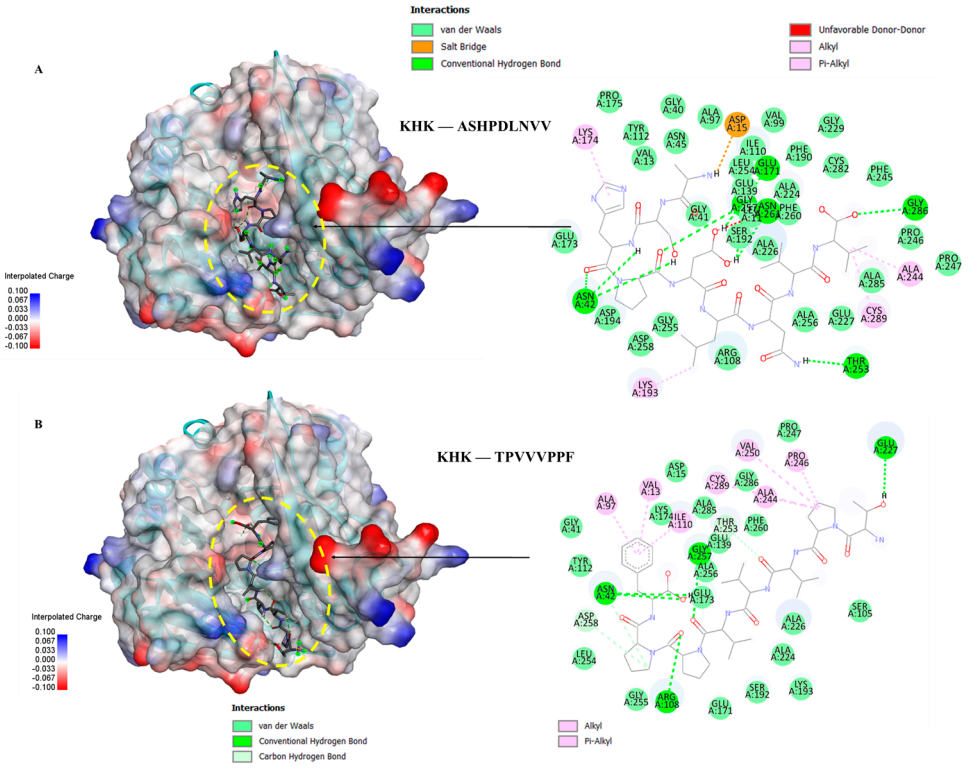

Figure 6. Molecular docking of peptides ASHPDLNVV and TPVVVPPF with KHK: **(A)** Binding pose and docking interactions of ASHPDLNVV with KHK; **(B)** binding pose and docking interactions of TPVVVPPF with KHK.

 doi:10.20944/preprints202504.0794.v1

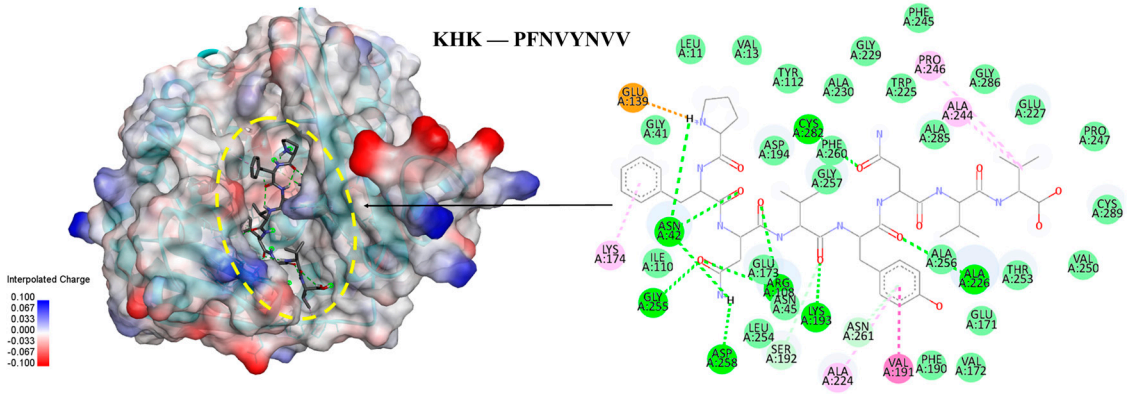

Figure 7. Molecular docking of PFNVYNVV peptide with KHK: Binding pose and docking interactions of ASHPDLNVV with KHK.

4. Discussion

Hepatic steatosis, commonly known as fatty liver, is defined by the abnormal accumulation of lipids, particularly triglycerides, within hepatocytes. It serves as a primary pathological feature of MASLD and is closely associated with components of the metabolic syndrome [3,27]. Hepatic steatosis poses a serious threat to individual health and represents a major challenge to public health systems worldwide. Despite progress in metabolic disease management, no FDA-approved drugs specifically target hepatic steatosis. Current treatments rely on lifestyle changes, while available medications offer limited benefits and may cause side effects [13]. Given these challenges, interest is growing in functional food components like bioactive proteins and peptides.

Goat milk, often considered a superior alternative to cow milk, has garnered attention for its health benefits. Goat whey proteins are known for their therapeutic effects, including immunomodulatory, anti-inflammatory, antioxidant, antimicrobial, and anti-cancer properties [18]. Therefore, this study aims to investigate the hepatoprotective effects of GWPH in a HFCS-induced murine model of hepatic steatosis and elucidate the underlying mechanisms involved in combating this condition.

Previous studies have shown that long-term HFCS consumption contributes to obesity, leading to increased body weight, fat accumulation, and elevated triglyceride levels [28,29]. In the present study, 8 weeks of HFCS feeding resulted in significant increases in body weight, liver weight, and visceral fat deposition in eWAT and prWAT (Table 1 and Figure 1). In contrast, GWPH-treated mice for 8 weeks alongside HFCS markedly reduced body weight gain, liver weight and visceral adiposity. Therefore, our findings indicated that GWPH mitigated HFCS-induced obesity. These results are consistent with the other studies using protein hydrolysates derived from whey proteins [19], bovine α-lactalbumin [30], *Litopenaeus vannamei* waste [31], herring milt [32] and synthetic oligopeptides [22,23] in murine models of diet-induced obesity and fatty liver disease.

The hepatoprotective effect of GWPH was evaluated by assessing serum levels of liver injury markers, ALT and AST. GWPH treatment significantly lowered these enzyme levels, indicating a notable improvement in liver function and attenuation of HFCS induced hepatic injury (Figure 2A). These results are consistent with a previous study by Wayal et al., (2025), where chicken meat hydrolysate demonstrated significant hepatoprotective effects against drug-induced liver injury [33]. Interestingly, the effects of GWPH on serum lipid profiles were less pronounced. GWPH treatment did not significantly alter serum levels of TG, TC, and VLDL compared to the HFCS-fed control group. However, a significant reduction in TC levels was observed in the GWPH30 group, suggesting a selective lipid modulating effect (Figure 2A). Previous studies have indicated that impaired lipid exports, particularly reduced VLDL secretion, contribute to hepatic TG accumulation. This effect is exacerbated by enhanced *de novo* lipogenesis (DNL), ultimately promoting the development and progression of hepatic steatosis [34,35]. Consistent with these findings, our results indicate that

 doi:10.20944/preprints202504.0794.v1

treatment GWPH, especially the GWPH03 and GWPH1030 fractions, markedly attenuated hepatic steatosis and ameliorated liver histological alterations compared to the Control group (Figure 4A, B). Furthermore, as illustrated in Figure 4C, Control group exhibited significantly elevated hepatic TG and VLDL levels. In contrast, GWPH-treated groups, most notably GWPH1030 showed a significant reduction in hepatic TG and VLDL levels when compared to the Control group, suggesting an improvement in hepatic lipid metabolism and export.

T2DM is a crucial metabolic abnormality closely linked to hepatic steatosis, together they exacerbate progression of MASLD [36]. Prior studies have reported that protein hydrolysates derived from black bean (*Phaseolus vulgaris L.)* [37] and pea protein [38] exhibit hypoglycemic effects by lowering fasting blood glucose levels and improving glucose tolerance in both human clinical trials and murine models of diet-induced diabetes. Similarly, camel milk protein hydrolysates have been shown to ameliorate hyperglycemia and hyperlipidemia in diabetic rats, suggesting their potent antihyperglycemic activity [39]. In line with these findings, our study showed that 8-week GWPH supplementation alongside HFCS intake significantly reduced FBG levels in all treatment groups, except GWPH0310 (Figure 3A). Additionally, GWPH-treated groups demonstrated improved glucose tolerance during the OGTT, with lower blood glucose levels and a significantly reduced AUC compared to the Control group (Figure 3B, C), indicating enhanced glucose homeostasis.

Excessive consumption of lipogenic sugars, such as fructose, contributes to the development of various metabolic disorders, including fatty liver disease [40]. Unlike glucose, fructose bypasses key regulatory steps and is rapidly phosphorylated by KHK to fructose-1-phosphate, resulting in ATP depletion and uncontrolled activation of lipid synthesis pathways. KHK is a critical enzyme in fructose metabolism, and its inhibition could be a potential therapeutic target for treating diet-induced metabolic disorders [6,26]. Prior in-silico study [41] and preclinical investigations using mouse and human liver models [42] have shown that the inhibition of KHK can reduced fructose induced hepatic steatosis and alleviate associated metabolic abnormalities. In line with these findings, our study identified five peptides (KYDSVLAV, EPQLHPF, ASHPDLNVV, TPVVVPPF and PFNVYNVV) from various molecular weight fractions of GWPH and evaluated for KHK inhibitory potential via molecular docking. All five peptides exhibited distinct binding energies, docking poses and key inter-actions with active site residues toward KHK (Table 2, Figure 5–Figure 7). Notably, PFNVYNVV exhibited the strongest binding affinity (–9.6 kcal/mol), surpassing Compound 14 [26], and mimicked its docking pose and interaction profile, suggesting its promise as a competitive KHK inhibitor.

5. Conclusions

In summary, this study is the first to demonstrate that GWPH effectively attenuates HFCS-induced hepatic steatosis, mitigates body weight gain and visceral adiposity, alleviates liver injury, enhances glucose homeostasis, and regulates hepatic lipid metabolism in mice. Notably, peptides derived from GWPH, especially PFNVYNVV, exhibited strong binding affinity toward KHK, suggesting potential as competitive inhibitors of fructose metabolism (Figure 8). These findings highlight the therapeutic potential of GWPH and its peptides in managing hepatic steatosis and related metabolic disorders. However, future studies should focus on the direct evaluation of these peptides *in-vivo*, investigate their molecular mechanisms, and validate KHK inhibition through enzymatic and structural analyses. Assessing their pharmacokinetics, bioavailability, and safety will also be crucial for advancing toward clinical application.

 doi:10.20944/preprints202504.0794.v1

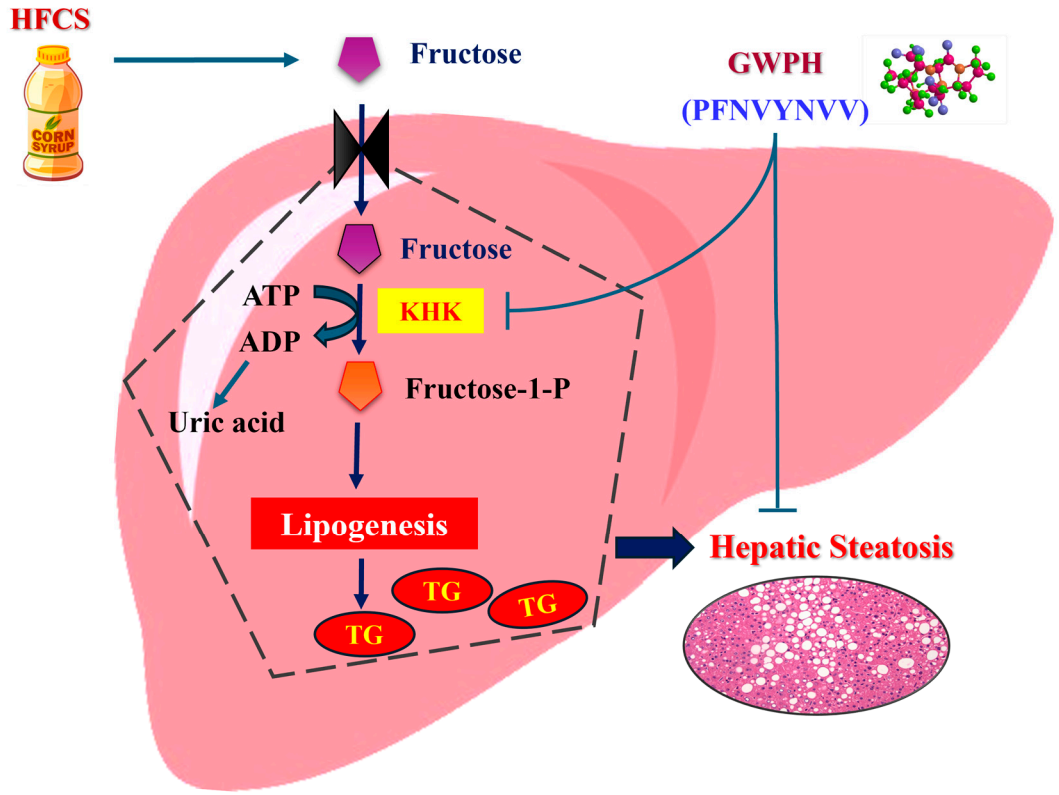

Figure 8. Schematic illustration of the proposed molecular mechanisms by which GWPH and its derived peptide (PFNVYNVV) mitigate HFCS-induced hepatic steatosis.

Supplementary Materials: The following supporting information can be downloaded at the website of this paper posted on Preprints.org. Figure S1: 3D structure of Lys-Tyr-Asp-Ser-Val-Leu-Ala-Val (KYDSVLAV) peptide; Figure S2: 3D structure of Glu-Pro-Gln-Leu-His-Pro-Phe (EPQLHPF) peptide; Figure S3: 3D structure of Ala-Ser-His-Pro-Asp-Leu-Asn-Val-Val (ASHPDLNVV) peptide; Figure S4: 3D structure of Thr-Pro-Val-Val-Val-Pro-Pro-Phe (TPVVVPPF) peptide; Figure S4: 3D structure of Thr-Pro-Val-Val-Val-Pro-Pro-Phe (TPVVVPPF) peptide; Figure S5: 3D structure of Pro-Phe-Asn-Val-Tyr-Asn-Val-Val (PFNVYNVV) peptide; Figure S6: Crystal structure of KHK (PDB ID: 2HLZ): Chains A, B, C, D: Ketohexokinase (KHK); Resolution: 1.85 Å.

Author Contributions: Conceptualization, C.-H.S. and C.-C.H.; methodology, C.-H.S. and C.-C.H.; software, V.W. and C.-C.H.; validation, C.-H.S., V.W. and C.-C.H.; formal analysis, C.-H.S., and V.W.; investigation, C.-H.S.; resources, C.-C.H.; data curation, C.-H.S.; writing—original draft preparation, C.-H.S. and V.W.; writing—review and editing, V.W. and C.-C.H.; visualization, C.-H.S. and V.W.; supervision, C.-C.H.; project administration, C.-C.H.; funding acquisition, C.-C.H.. All authors have read and agreed to the published version of the manuscript.

Funding: This research was funded by the National Science and Technology Council, Taiwan, grant number MOST 103-2221-E-029-017 and the Ministry of Agriculture, Taiwan, grant number 105AS-2.1.5-AD-U1.

Data Availability Statement: The original contributions presented in this study are included in the article/supplementary material. Further inquiries can be directed to the corresponding author(s).

Acknowledgments: We are deeply grateful to Prof. Dr. Chang-Chi Hsieh and Dr. Vipul Wayal for their invaluable guidance, support, and expertise in fatty liver disease research. Their insights significantly contributed to our study design and interpretation of findings. We also extend our appreciation to Dr. Hsieh's lab at Tunghai University and Central Clinic & Hospital for providing the necessary facilities and resources that made this research possible.

Conflicts of Interest: The authors declare no conflicts of interest.

 doi:10.20944/preprints202504.0794.v1

Abbreviations

The following abbreviations are used in this manuscript:

HFCS	High-fructose corn syrup
GWPH	Goat whey protein hydrolysate
TG	Triglycerides
hTG	Hepatic triglycerides
TC	Total cholesterol
VLDL	Very low-density lipoprotein
hVLDL	Hepatic very low-density lipoprotein
ALT	Alanine aminotransferase
AST	Aspartate aminotransferase
FBG	Fasting blood glucose
KHK	Ketohexokinase
BCA	Bicinchoninic acid
BW	Body weight
eWAT	Epididymal white adipose tissue
prWAT	Perirenal white adipose tissue

References

1. Orabi, D.; Berger, N.A.; Brown, J.M. Abnormal Metabolism in the Progression of Nonalcoholic Fatty Liver Disease to Hepatocellular Carcinoma: Mechanistic Insights to Chemoprevention. *Cancers (Basel)* **2021**, *13*, 3473.
2. Paul, B.; Lewinska, M.; Andersen, J. B. Lipid alterations in chronic liver disease and liver cancer. *JHEP Reports* **2022**, *4*, 100479.
3. Zarghamravanbakhsh, P.; Frenkel, M.; Poretsky, L. Metabolic causes and consequences of nonalcoholic fatty liver disease (NAFLD). *Metabolism Open* **2021**, *12*, 100149.
4. Kang, C. C.; Wang, T. E.; Liu, C. Y.; Chen, M. J.; Wang, H. Y.; Chang, C. W.; Chang, C. W. Update on Imaging-based Noninvasive Methods for Assessing Hepatic Steatosis in Nonalcoholic Fatty Liver Disease. *J. Med. Ultrasound* **2024**, *32*, 116-120.
5. Chen, L. From metabolic dysfunction-associated fatty liver disease to metabolic dysfunction-associated steatotic liver disease: Controversy and consensus. *World J. Hepatol*. **2023**, *15*, 1253-1257.
6. Ferreira, J. C.; Villanueva, A. J.; Fadl, S.; Al Adem, K.; Cinviz, Z. N.; Nedyalkova, L.; Cardoso, T. H. S.; Andrade, M. E.; Saksena, N. K.; Sensoy, O.; et al. Residues in the fructose-binding pocket are required for ketohexokinase-A activity. *J. Biol. Chem.* **2024**, *300*, 107538.
7. Jensen, T.; Abdelmalek, M. F.; Sullivan, S.; Nadeau, K. J.; Green, M.; Roncal, C.; Nakagawa, T.; Kuwabara, M.; Sato, Y.; Kang, D. H.; et al. Fructose and sugar: A major mediator of non-alcoholic fatty liver disease. *J. Hepatol.* **2018**, *68*, 1063-1075.
8. Lodge, M.; Dykes, R.; Kennedy, A. Regulation of Fructose Metabolism in Nonalcoholic Fatty Liver Disease. *Biomolecules* **2024**, *14*, 845.
9. Kazierad, D. J.; Chidsey, K.; Somayaji, V. R.; Bergman, A. J.; Birnbaum, M. J.; Calle, R. A. Inhibition of ketohexokinase in adults with NAFLD reduces liver fat and inflammatory markers: A randomized phase 2 trial. *Med*. **2021**, *2*, 800-813.e803.
10. Meyers, A. M.; Mourra, D.; Beeler, J. A. High fructose corn syrup induces metabolic dysregulation and altered dopamine signaling in the absence of obesity. *PLoS ONE* **2017**, *12*, e0190206.
11. Rippe, J. M.; Angelopoulos, T. J. Fructose-Containing Sugars and Cardiovascular Disease. *Advances in Nutrition* **2015**, *6*, 430-439.
12. Li, Y. C.; Hsieh, C. C. Lactoferrin dampens high-fructose corn syrup-induced hepatic manifestations of the metabolic syndrome in a murine model. *PLoS ONE* **2014**, *9*, e97341.
13. Takahashi, Y.; Sugimoto, K.; Inui, H.; Fukusato, T. Current pharmacological therapies for nonalcoholic fatty liver disease/nonalcoholic steatohepatitis. *World J. Gastroenterol.* **2015**, *21*, 3777-3785.

 doi:10.20944/preprints202504.0794.v1

14. Zaky, A. A.; Simal-Gandara, J.; Eun, J. B.; Shim, J. H.; Abd El-Aty, A. M. Bioactivities, Applications, Safety, and Health Benefits of Bioactive Peptides from Food and By-Products: A Review. *Front. Nutr.* **2021**, *8*, 815640.
15. Wang, S.; Zhao, M.; Fan, H.; Wu, J. Emerging proteins as precursors of bioactive peptides/hydrolysates with health benefits. *Curr. Opin. Food Sci.* **2022**, *48*, 100914.
16. Daliri, E.B.-M.; Oh, D.H.; Lee, B.H. Bioactive Peptides. *Foods* **2017**, *6*, 32.
17. Hu, Y.; Luo, H.; Netala, V.R.; Li, H.; Zhang, Z.; Hou, T. Comprehensive Review of Biological Functions and Therapeutic Potential of Perilla Seed Meal Proteins and Peptides. *Foods* **2025**, *14*, 47
18. QH, A. L.; Al-Saadi, J. S.; Al-Rikabi, A. K. J.; Altemimi, A. B.; Hesarinejad, M. A.; Abedelmaksoud, T. G. Exploring the health benefits and functional properties of goat milk proteins. *Food Sci. Nutr.* **2023**, *11*, 5641-5656.
19. Wang, K.; Fu, Z.; Li, X.; Hong, H.; Zhan, X.; Guo, X.; Luo, Y.; Tan, Y. Whey protein hydrolysate alleviated atherosclerosis and hepatic steatosis by regulating lipid metabolism in apoE-/- mice fed a Western diet. *Food Res. Int.* **2022**, *157*, 111419.
20. Sansi, M. S.; Iram, D.; Vij, S.; Kapila, S.; Meena, S. *In vitro* biosafety and bioactivity assessment of the goat milk protein derived hydrolysates peptides. *J. Food Saf.* **2023**, *43*, e13061.
21. Friedewald, W. T.; Levy, R. I.; Fredrickson, D. S. Estimation of the concentration of low-density lipoprotein cholesterol in plasma, without use of the preparative ultracentrifuge. *Clin. Chem.* **1972**, *18*, 499-502.
22. Wayal, V.; Hsieh, C. C. Bioactive dipeptides mitigate high-fat and high-fructose corn syrup diet-induced metabolic-associated fatty liver disease via upregulation of Nrf2/HO-1 expressions in C57BL/6J mice. *Biomed. Pharmacother.* **2023**, *168*, 115724.
23. Wayal, V.; Wang, S. D.; Hsieh, C. C. Novel bioactive peptides alleviate Western diet-induced MAFLD in C57BL/6J mice by inhibiting NLRP3 inflammasome activation and pyroptosis via TLR4/NF-kappaB and Keap1/Nrf2/HO-1 signaling pathways. *Int. Immunopharmacol.* **2025**, *148*, 114177.
24. Morris GM, Huey R, Lindstrom W, et al. AutoDock4 and AutoDockTools4: Automated docking with selective receptor flexibility. *J Comput. Chem.* **2009**, *30*, 2785-2791.
25. Dassault Systems BIOVIA, Discovery Studio Visualizer [Version 4.5], San Diego: Dassault Systems BIOVIA, **2022**. Available from: https://discover.3ds.com/discovery-studio-visualizer.
26. Zhu, G.; Li, J.; Lin, X.; Zhang, Z.; Hu, T.; Huo, S.; Li, Y. Discovery of a Novel Ketohexokinase Inhibitor with Improved Drug Distribution in Target Tissue for the Treatment of Fructose Metabolic Disease. *J. Med. Chem.* **2023**, *66*, 13501-13515.
27. Rao, G.; Peng, X.; Li, X.; An, K.; He, H.; Fu, X.; Li, S.; An, Z. Unmasking the enigma of lipid metabolism in metabolic dysfunction-associated steatotic liver disease: from mechanism to the clinic. *Front. Med. (Lausanne)* **2023**, 10, 1294267.
28. Bocarsly, M. E.; Powell, E. S.; Avena, N. M.; Hoebel, B. G. High-fructose corn syrup causes characteristics of obesity in rats: increased body weight, body fat and triglyceride levels. *Pharmacol. Biochem. Behav.* **2010**, *97*, 101-106.
29. Bray, G. A.; Nielsen, S. J.; Popkin, B. M. Consumption of high-fructose corn syrup in beverages may play a role in the epidemic of obesity. *Am. J. Clin. Nutr.* **2004**, *79*, 537-543.
30. Gao, J.; Song, J.; Du, M.; Mao, X. Bovine α-Lactalbumin Hydrolysates (α-LAH) Ameliorate Adipose Insulin Resistance and Inflammation in High-Fat Diet-Fed C57BL/6J Mice. *Nutrients* **2018**, *10*, 242.
31. Hadavi, M.; Najdegerami, E. H.; Nikoo, M.; Nejati, V. Protective effect of protein hydrolysates from *Litopenaeus vannamei* waste on oxidative status, glucose regulation, and autophagy genes in non-alcoholic fatty liver disease in Wistar rats. *Iran J. Basic Med. Sci.* **2022**, *25*, 954-963.
32. Wang, Y.; Nair, S.; Gagnon, J. Herring Milt and Herring Milt Protein Hydrolysate Reduce Weight Gain and Improve Insulin Sensitivity and Pancreatic Beta-Cell Function in Diet-Induced Obese Mice. *Curr. dev. nutr.* **2020**, *4*, nzaa063_097.
33. Wayal, V.; Tsai, Z.-E.; Lin, Y.-H.; Lai, Y.-H.; Wang, S.-D.; Hsieh, C.-C. Chicken meat hydrolysate improves acetaminophen-induced liver injury by alleviating oxidative stress via modulation in Keap1/Nrf2/HO-1 signaling in BALB/c mice. *J. Agric. Food Res.* **2025**, *21*, 101863.

 doi:10.20944/preprints202504.0794.v1

34. Matsuzaka, T.; Shimano, H. Molecular mechanisms involved in hepatic steatosis and insulin resistance. *J. Diabetes Investig*. **2011**, *2*, 170-175.
35. Heeren, J.; Scheja, L. Metabolic-associated fatty liver disease and lipoprotein metabolism. *Mol. Metab*. **2021**, *50*, 101238.
36. Zheng, H.; Sechi, L. A.; Navarese, E. P.; Casu, G.; Vidili, G. Metabolic dysfunction-associated steatotic liver disease and cardiovascular risk: a comprehensive review. *Cardiovasc. Diabetol.* **2024**, *23*, 346.
37. Mojica, L.; Ramos-Lopez, A. S.; Sánchez-Velázquez, O. A.; Gómez-Ojeda, A.; Luevano-Contreras, C. Black bean (*Phaseolus vulgaris* L.) protein hydrolysates reduce acute postprandial glucose levels in adults with prediabetes and normal glucose tolerance. *J. Funct. Foods* **2024**, *112*, 105927.
38. Liao, W.; Cao, X.; Xia, H.; Wang, S.; Chen, L.; Sun, G. Pea protein hydrolysate reduces blood glucose in high-fat diet and streptozotocin-induced diabetic mice. *Front. Nutr.* **2023**, *10*, 1298046.
39. Kilari, B. P.; Mudgil, P.; Azimullah, S.; Bansal, N.; Ojha, S.; Maqsood, S. Effect of camel milk protein hydrolysates against hyperglycemia, hyperlipidemia, and associated oxidative stress in streptozotocin (STZ)-induced diabetic rats. *J. Dairy Sci.* **2021**, *104*, 1304-1317.
40. Kazierad, D. J.; Chidsey, K.; Somayaji, V. R.; Bergman, A. J.; Birnbaum, M. J.; Calle, R. A. Inhibition of ketohexokinase in adults with NAFLD reduces liver fat and inflammatory markers: A randomized phase 2 trial. *Med.* **2021**, *2*, 800-813.e803.
41. Shepherd, E. L.; Saborano, R.; Northall, E.; Matsuda, K.; Ogino, H.; Yashiro, H.; Pickens, J.; Feaver, R. E.; Cole, B. K.; Hoang, S. A.; et al. Ketohexokinase inhibition improves NASH by reducing fructose-induced steatosis and fibrogenesis. *JHEP Reports* **2021**, *3*, 100217.
42. Futatsugi, K.; Smith, A. C.; Tu, M.; Raymer, B.; Ahn, K.; Coffey, S. B.; Dowling, M. S.; Fernando, D. P.; Gutierrez, J. A.; Huard, K.; et al. Discovery of PF-06835919: A Potent Inhibitor of Ketohexokinase (KHK) for the Treatment of Metabolic Disorders Driven by the Overconsumption of Fructose. *J. Med. Chem*. **2020**, *63*, 13546-13560.